EPSC Abstracts
Vol. 5, EPSC2010-341, 2010
European Planetary Science Congress 2010

Estimation of visible, near-, and mid-infrared optical constants of dolomite

T. Roush, NASA Ames Research Center, Moffett Field, CA, USA (Ted.L.Roush@nasa.gov)

Abstract

The initial estimates of the optical constants of dolomite are presented for the ~0.4-5 μm wavelength region. These values provide the ability to undertake radiative transfer calculations relevant to quantitative abundance estimates of these materials in the Martian environment.

1. Introduction

Carbonate minerals are germane to questions involving volatile and climate history on Mars [e.g., [1,2]. In particular, the abundance of carbonate-bearing minerals can provide broad useful bounds on the amount of CO_2 out-gassed into the atmosphere over its history and their spatial distribution and mineralogy can yield constraints on the environments in which they were produced. Infrared spectral observations from aircraft and Earth-orbiting satellites provided evidence for the presence of carbonates in the Martian environment [1,3]. Infrared observations made from space craft near Mars were interpreted to indicate the presence of carbonates [4,5]. [5] associated the carbonates with the surface dust and interpreted the mineralogy as being consistent with magnesite ($MgCO_3$). Recent near-infrared observations from Mars orbit have been interpreted to show carbonate outcrops in restricted locations and again the favored carbonate is magnesite [6,7].

Quantitative estimates of the abundance of carbonates on Mars range from 0-3% [1], 2-5% [5], less than a few percent [8], and <10% [7]. With the growing evidence for magnesite on Mars additional quantitative estimates can be provided via theoretical modeling of the reflectance from the Martian surface. However, such modeling efforts rely upon optical constants of the candidate materials.

Calcite ($CaCO_3$) and dolomite ($(Ca,Mg)CO_3$) are identified in Asian [9] dust and Calcite in Saharan dust [10-13]. The importance of optical constants at visible and near-infrared wavelengths, as proxies for estimating the effects at infrared wavelengths, is beginning to be investigated [13].

The growing evidence for Mg-carbonates on Mars, the presence of calcite and dolomite in terrestrial aerosols, and general lack of optical constants for these materials in the visible- to mid-infrared (vmir, ~0.3-6 μm) has motivated a broader effort [14] to estimate the optical constants of calcite, dolomite, and magnesite in the vmir. Here I report the initial estimates of the optical constants for dolomite.

2. Available Data

In the near-infrared there is a lack of optical constants for dolomite. At infrared wavelengths the optical constants for dolomite were reported by [15-17]. Given the agreement among the [15] and [16] values and the fact that [15] studies all three carbonates under consideration for the broader study, I select to rely upon the [15] data for dolomite in the infrared.

There are several on-line digital spectral libraries that potentially contain dolomite reflectance spectra that can be used to estimate the optical constants of the carbonates in the VMIR [18-22]. Each library was searched for available data and a total of 23 possible samples were identified. All but one sample was eliminated due to the availability of only a single grain size, the presence of spectral features associated with other materials, the presence of odd spectral behavior, and/or lack of data at wavelengths that overlap with the infrared data. The reflectance spectra of the three grain size separates of this

remaining sample are shown in Figure 1.

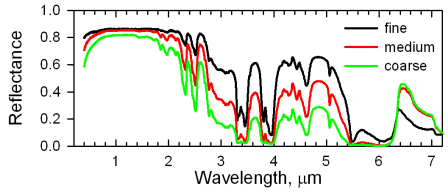

Figure 1. Reflectance spectra of dolomite sample C5-C of fine (<45 μm), medium (45-125 μm), and coarse (125-500 μm) grain size separates from the ASTER spectral library.

3. Analytical Approach

Here the approach of [23] is used. The basic approach is to use multiple grain sizes of the same sample and assume all grain sizes have the same composition. Unless independently known as a function of wavelength an additional assumption must be made regarding real index of refraction. A model of the interaction of light with particulates surfaces is used to iteratively determine the imaginary index by iteratively calculating the reflectance and comparing the result to the measured reflectance using a χ^2- criterion. The interested reader is referred to [23] for more details.

The model of Hapke [24,25] [1981, 1993] is used as presented in equations (1)–(6) of [26] and equations (1)–(4) of [27]. Scattering is assumed isotropic, h, the width of the opposition surge, is assumed to be 0.05, and Hapke's internal scattering parameter, s, is 0. The first two of these parameters require observations at multiple viewing geometries that were not obtained for the laboratory data used for these analyses. The third parameter is poorly characterized for natural materials and setting it to zero effectively forces the absorption coefficient to account for all the spectral behavior. The median grain size for each particle size separate is used for initially estimating the imaginary index of refraction.

Following [23] the imaginary indices are used to estimate the real index and this process is iterated until the values do not change significantly. The approach uses a subtractive Kramers-Konig analysis to determine the wavelength dependence of the real index. This is possible by using existing infrared data of [15] to estimate the wavelength behavior of the real index in the vmir region. [15] presents the dispersion analysis for data from both optical axes of dolomite at infrared wavelengths. Because the diffuse reflectance of the samples used in the current study is obtained from relatively fine grains, the contribution from each optical axis in the infrared is represented by an average.

Using the oscillator parameters and high frequency dielectric constants from [15], and assuming a 2 cm^{-1} spectral sampling that was not specified in [15], the real and imaginary indices of refraction for the range of the [15] data, 4000-20 cm^{-1}, the average of the crystallographic axes is shown in Figure 2.

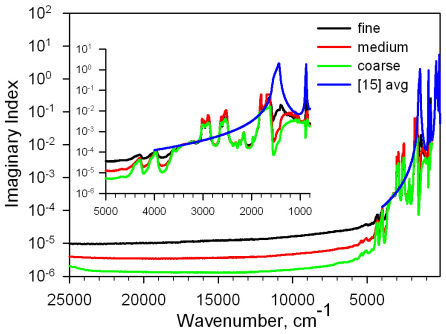

Figure 2. Imaginary Index of refraction calculated from [15] compared to the initial estimate from each individual grain size of the reflectance data. The inset shows the region of overlap between the data sets in the vmir and ir regions.

To create a single data set from the vmir reflectance measurements the coarsest grain size results are preferred, then the medium, and finally the finest grain size. This is due to the sensitivity of the largest grain size to weaker features [28]. However, in a few restricted wavelength regions, the coarsest grain size reflectance measurement is saturated (reflectance <0.02), and the medium grain size imaginary indices are used. In the regions were the medium grain size reflectance is saturated, then the imaginary indices estimated from finest grain size reflectance are used. The imaginary indices are combined with those calculated from [15] and then the Kramers-Kronig analysis is performed. The initial results for the real and imaginary indices are shown in Figure 3.

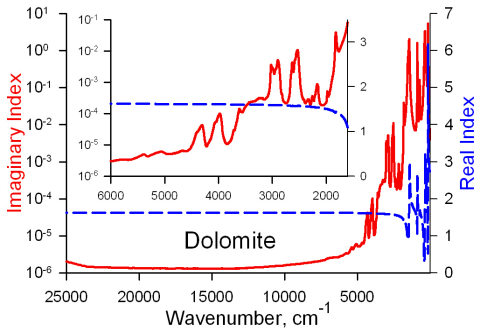

Figure 3. The real (blue, right axis) and imaginary index (red, left axis) of refraction of dolomite. The inset shows the region of overlap between the values derived from the reflectance measurements and those calculated from [15].

4. Summary and Conclusions

The initial estimates of the optical constants of dolomite are presented. These values, along with those for magnesite [14], begin providing the ability to undertake radiative transfer calculations relevant to quantitiative abundance estimates of these materials in the Martian atmosphere.

Acknowledgements

This research is sponsored by NASA's Planetary Geology and Geophysics Program.

References

[1] Pollack, J.B., et al. (1990) Thermal emission spectra of Mars (5.4-10.5 µm): Evidence for sulfates, carbonates, and hydrates, *J. Geophys. Res.*, 95, 14,595-14,627.

[2] Fanale, F. et at. (1992) Mars: Epochal climate change and volatile history, in *Mars*, H. Kieffer et al. Eds., Univ. Arizona Press, Tucson, AZ, USA, 1135-1179.

[3] Lellouch, E. et al. (2000) The 2.4-45 µm spectrum of Mars observed with the Infrared Space Observatory, *Planet. Sp. Sci.* 48, 1393-1405.

[4] Calvin, W. et al. (1994) Hydrous carbonates on Mars?: Evidence from Mariner 6/7 infrared spectrometer and ground-based telescopic spectra, *J. Geophys. Res.* 99, 14,659-14,675.

[5] Bandfield, J. et al. (2003) Spectroscopic Identification of Carbonate Minerals in the Martian Dust, *Science* 301, 1084-1087.

[6] Ehlmann, B. et al. (2008) (2008) Orbital identification of carbonate-bearing rocks on Mars, *Science* 322, 1828-1832.

[7] Palomba, E. et al. (2009) Evidence for Mg-rich carbonates on Mars from a 3.9 µm absorption feature, *Icarus* 203, 58-65.

[8] Bibring, J-P., et al. (2005) Mars Surface Diversity as Revealed by the OMEGA/Mars Express Observations, *Science* 307, 1576-1581.

[9] Jeong, G. (2008) Bulk and single-particle mineralogy of Asian dust and a comparison with its source soils, *J. Geophys. Res*. 113, D02208, doi: 10.1029/2007JD008606.

[10] Glaccum, R. and J. Prospero (1980) Saharan Aerosols over the tropical North Atlantic: Mineralogy, *Mar. Geol.* 37, 295– 321.

[11] Avila, A. et al. (1997) Mineralogical composition of African dust delivered by red rains over northeastern Spain, *J. Geophys. Res.* 102, 21,977-21,996.

[12] Reid, E. et al. (2003) Characterization of African dust transported to Puerto Rico by individual particle and size segregated bulk analysis, *J. Geophys. Res*. 108, doi: 10.1029/2002JD002935.

[13] Hansell, R. et al. (2010) A Sensitivity Study on the Effects of Particle Chemistry, Asphericity and Size on the Mass Extinction Efficiency of Mineral Dust in the Terrestrial Atmosphere: From the Near to Thermal IR, *Atmos. Chem. Phys. J.*, in revision.

[14] Roush, T.L. (2009) Estimated optical constants of magnesite ($MgCO_3$) 40th Lunar Planetary Sci. Conf., abstract 1080, Lunar and Planetary Institute, Houston, Texas.

[15] Hellwege, K.H., et al., (1970) Zwei-Phononen-Absorptionsspektren un dispersion der schwingungszweige in kristallen der kalkspatstruktur, *Z. Physik.*, 232, 61-86.

[16] Querry, M. (1987) Optical Constants of Minerals and Other Materials from the Millilmeter To the Ultraviolet, Contractor report CRDEC-CR-88009, U.S. Army Chemical Research, Development and Engineering Center, Aberdeen Proving Ground, Maryland USA, 333pp.

[17] Posch et al., (2007) Carbonates in space: the challenge of low-temperature data, *Ap. J.*, 668, 993-1000.

[18] pds-geciences.wustl.edu/MROCRISM SpectralLibrary

[19] lf314-rlds.geo.brown.edu

[20] speclib.jpl.nasa.gov

[21] Clark, R. et al. (2003) USGS digital spectral library splib05a, U.S. Geol. Surv. Open File Report, pp. 3 – 395.

[22] Cloutis, E. (2008) Hyperspectral optical sensing for extraterrestrial reconnaissance laboratory, http://psf.uwinnipeg.ca/Sample_Database.html/Mineral_database_latest_1.doc.

[23] Roush, T., et al. (2007) Estimated optical constants of Gypsum in the regions of weak absorptions: Application of scattering theories and comparisons to independent measurements, *J. Geophys. Res.-Planets*, 112, E10003, doi:10.1029/2007JE002920.

[24] Hapke, B, (1981) Bidirectional reflectance spectroscopy: 1. Theory, *J. Geophys. Res.*, 86, 3039-3054.

[25] Hapke, B. (1993) *Theory of Reflectance and Emittance Spectroscopy*, Cambridge Univ. Press, New York, NY, 455pp.

[26] Roush, T. (1994) Charon: More Than Water Ice?, *Icarus,* 108, 243-254.

[27] Cruikshank, D., et al. (1997) *The Surfaces of Pluto and Charon*, in *Pluto and Charon*, D.J. Tholen and A. Stern, Eds., University of Arizona Press, 221-267.

[28] Pieters, C. (1983) Strength of mineral absorption features in the transmitted component of near-infrared reflected light - First results from RELAB, *J. Geophys. Res.* 88, 9534-9544.